Pediatr Radiol (2014) 44:787–794
DOI 10.1007/s00247-014-2899-y

ORIGINAL ARTICLE

Computed tomography depiction of small pediatric vessels with model-based iterative reconstruction

Gonca Koc · Jesse L. Courtier · Andrew Phelps · Peter A. Marcovici · John D. MacKenzie

Received: 26 August 2013 / Revised: 31 December 2013 / Accepted: 23 January 2014 / Published online: 16 February 2014

Abstract
Background Computed tomography (CT) is extremely important in characterizing blood vessel anatomy and vascular lesions in children. Recent advances in CT reconstruction technology hold promise for improved image quality and also reductions in radiation dose. This report evaluates potential improvements in image quality for the depiction of small pediatric vessels with model-based iterative reconstruction (Veo™), a technique developed to improve image quality and reduce noise.
Objective To evaluate Veo™ as an improved method when compared to adaptive statistical iterative reconstruction (ASIR™) for the depiction of small vessels on pediatric CT.
Materials and methods Seventeen patients (mean age: 3.4 years, range: 2 days to 10.0 years; 6 girls, 11 boys) underwent contrast-enhanced CT examinations of the chest and abdomen in this HIPAA compliant and institutional review board approved study. Raw data were reconstructed into separate image datasets using Veo™ and ASIR™ algorithms (GE Medical Systems, Milwaukee, WI). Four blinded radiologists subjectively evaluated image quality. The pulmonary, hepatic, splenic and renal arteries were evaluated for the length and number of branches depicted. Datasets were compared with parametric and non-parametric statistical tests.
Results Readers stated a preference for Veo™ over ASIR™ images when subjectively evaluating image quality criteria for vessel definition, image noise and resolution of small anatomical structures. The mean image noise in the aorta and fat was significantly less for Veo™ vs. ASIR™ reconstructed images. Quantitative measurements of mean vessel lengths and number of branches vessels delineated were significantly different for Veo™ and ASIR™ images. Veo™ consistently showed more of the vessel anatomy: longer vessel length and more branching vessels.
Conclusion When compared to the more established adaptive statistical iterative reconstruction algorithm, model-based iterative reconstruction appears to produce superior images for depiction of small pediatric vessels on computed tomography.

Keywords Computed tomography · Image reconstruction · Pediatric · CT angiography · Image quality · Model-based iterative reconstruction

G. Koc · J. L. Courtier · A. Phelps · P. A. Marcovici · J. D. MacKenzie (✉)
Department of Radiology and Biomedical Imaging
UCSF Benioff Children's Hospital, 505 Parnassus Ave.
San Francisco, CA 94143-0628, USA
e-mail: john.mackenzie@ucsf.edu

Introduction

Computed tomography (CT) is an important imaging modality that plays a central role in the management of pediatric patients [1]. Multiple factors contribute to the creation of high-quality CT images and a clear relationship exists between the amount of ionizing radiation dose delivered and the diagnostic quality of CT images [2–4]. In addition, new technologies continue to have an impact on the performance of CT and it is important to test and report the benefits that these technologies may confer for the imaging care of pediatric patients. Recently, image reconstruction algorithms have been modified to potentially improve image quality while substantially reducing dose [5–7]. Although the concept of model-based iterative reconstruction (MBIR) is well described, it is only recently that advanced computer hardware and software have been available to provide relatively rapid reconstruction times and leverage this reconstruction algorithm for clinical use [8–10].

The features of MBIR that contribute to enhanced image quality include more precise noise modeling and more efficient utilization of scan data by modeling the entire geometry of the X-ray beam: anode, actual focal spot size, attenuation

within patient and capture by detector [11]. This has the potential to produce images with less noise over a wide range of tissue types and densities. In comparison, although adaptive statistical iterative reconstruction (ASIR™) algorithm has some ability to model system optics, ASIR™ focuses on modeling noise statistics and photons [12]. Superior spatial resolution has also been reported for MBIR images through phantom study [13, 14]. This has important implications for resolution-dependent diagnostic tasks, which include both CT angiography and pediatric CT, where the features of interest are inherently smaller.

The goal of our study was to test the ability of a commercialized MBIR technique (Veo™) to depict pediatric vessel anatomy on CT angiography and compare this with another more established reconstruction algorithm (ASiR™). Although two recent studies have evaluated Veo™ for use in children (assessment of image quality on non-contrast enhanced CT of the lungs [14] and another has evaluated the potential for reduced-dose CT [15]), no study has evaluated potential improvements in CT angiography using dedicated pediatric CT protocols. Pediatric patients are ideal to study due to the inherent challenges in imaging their smaller anatomy with high image quality. We hypothesize that Veo™ has the potential to improve the depiction of small vessel anatomy over ASIR™.

Materials and methods

Patients

Seventeen consecutive pediatric patients were enrolled in this study (mean age: 3.4 years, range: 2 days to 10.0 years; 6 girls, 11 boys). The children were referred to our department for enhanced CT work-up of pediatric diseases either affecting the blood vessels or requiring an anatomical depiction of the vascular anatomy. The study was HIPAA compliant and approved by our institutional review board.

CT protocols

CT scans were obtained with a 64-row MDCT system (GE Healthcare-Discovery CT750 HD, Milwaukee, WI) after the administration of iodinated contrast material (2 mL/kg of Omnipaque 350; GE Healthcare, Princeton, NJ) injected with a power injector through either a peripheral intravenous catheter or central venous power injectable catheter with the rate adjusted to the patient's size at 0.3 – 3 mL/s. Injection and CT scan parameters followed a pediatric CT angiography protocol that adjusts CT parameters based on the weight of the child (Table 1). Since the Veo™ technology has been recently deployed at our institution, we have not yet attempted to adjust scan parameters to take advantage of the potential dose reduction with Veo™. The scans were obtained with parameters optimized for our current ASIR™ protocol that had been successfully deployed over 2 years preceding this study.

Raw data were reconstructed into axial 0.625-mm slices using the Veo™ and ASIR™ reconstruction engines (GE Medical Systems, Milwaukee, WI) for MBIR and ASIR™, respectively. ASIR™ images were created with soft-tissue 30% ASIR™ blended with 70% filtered back projection reconstruction. No reconstruction parameter adjustments are possible with the current clinically available Veo™ reconstruction engine. The 0.625-mm thin-slice datasets were then transferred to a clinical workstation (AW Server; GE Healthcare, Milwaukee, WI) and reformatted axial images (3-mm thick with 2-mm spacing) were created for the subjective reader assessment of image quality.

Table 1 CT scan parameters were modified in a systematic matter based on the patient's weight (weight range) to adjust/optimize the ionizing radiation dose and image quality. Rotation time=0.5 s and detector configuration=64×0.625 mm were kept constant for all scans. *No.* number of patients per category, *kg* kilograms, *kVp* tube voltage, *mA max* maximum tube current allowed using automatic tube current modulation, *inj.* injection, *s* seconds, *mm* millimeters

Weight-based CT scan protocol

No.	Weight range (kg)	kVp	mA max	Noise index	Inj. delay (s)	Slice thickness (mm)	Pitch
4	6–7.5	80	110	10	5	2.5	0.9
3	7.5–9.5	100	95	10	5	2.5	1.375
3	9.5–11.5	100	110	10	10	2.5	1.375
2	11.5–14.5	100	125	12	15	3.75	1.375
3	14.5–18.5	100	140	12	20	3.75	1.375
	18.5–22.5	100	150	12	20	3.75	1.375
1	22.5–31.5	100	155	14	20	3.75	1.375
1	31.5–40.5	100	170	14	25	3.75	1.375
	>40.5	100	200	16	30	3.75	1.375

Subjective assessment

Image datasets were randomly coded and scan parameters removed including series identifiers (e.g., Veo™ and ASIR™) and viewed on a clinical picture-archiving and communication system (PACS) diagnostic workstation (Impax ES version 4; Agfa Technical Imaging Systems, Ridgefield Park, NJ) with clinical grade high-resolution monitors (NEC MultiSync LCD2090UXi-BK- 20 in. LCD display; Ampronix, Irvine, CA, USA). Four board-certified radiologists with 2, 2, 5 and 8 years of post-residency experience, respectively, independently evaluated the image datasets. Datasets were displayed on side-by-side monitors with the slices of the blinded Veo™ and ASIR™ images locked for easy comparison while scrolling through the image stacks. The readers assigned a score for the overall quality of each CT study based on a 5-point Likert scale (1=nondiagnostic, 2=limited evaluation of arteries, 3=adequate to make a diagnosis, 4=good depiction of arteries with some artifact or limitation in technique, 5=excellent technique and visualization of arteries). For each patient, readers compared the blinded Veo™ and ASIR™ datasets and provided a preference for the following parameters: vessel depiction, resolution of small anatomical structures and qualitative image noise (Fig. 1). Images were evaluated using mediastinum and lung window settings; however, the radiologists were allowed to change the window level and width as per their preference. Evaluation for vessel depiction was based on contrast resolution and visual sharpness of branch vessels. Small anatomical structures used to compare both Veo™ and ASIR™ datasets included lung bronchioles, lymph nodes and adrenal glands. Relative absence of/less image noise was judged by examining tissues such as subcutaneous fat where quantum mottle is easily discernable.

Objective image analysis

Image noise was measured by calculating the standard deviation of Hounsfield unit scale in a region of interest (ROI) on three tissue types: lumen of the descending thoracic aorta (ROI area=0.5 cm^2) at the level of carina, subcutaneous fat of the anterior thorax/axillae (1.0 cm^2) and the right paraspinal muscle (1.0 cm^2). The ROI was identical in placement, shape and size for the same patient on both the Veo™ and ASIR™ images. The ROI was placed at an area that visually appeared to contain a homogenous region of tissue.

Vessel lengths were measured for the apical segmental branch of the right upper lobe pulmonary (PA), right hepatic (HA), upper pole splenic (SA) and renal arteries (RA) on a

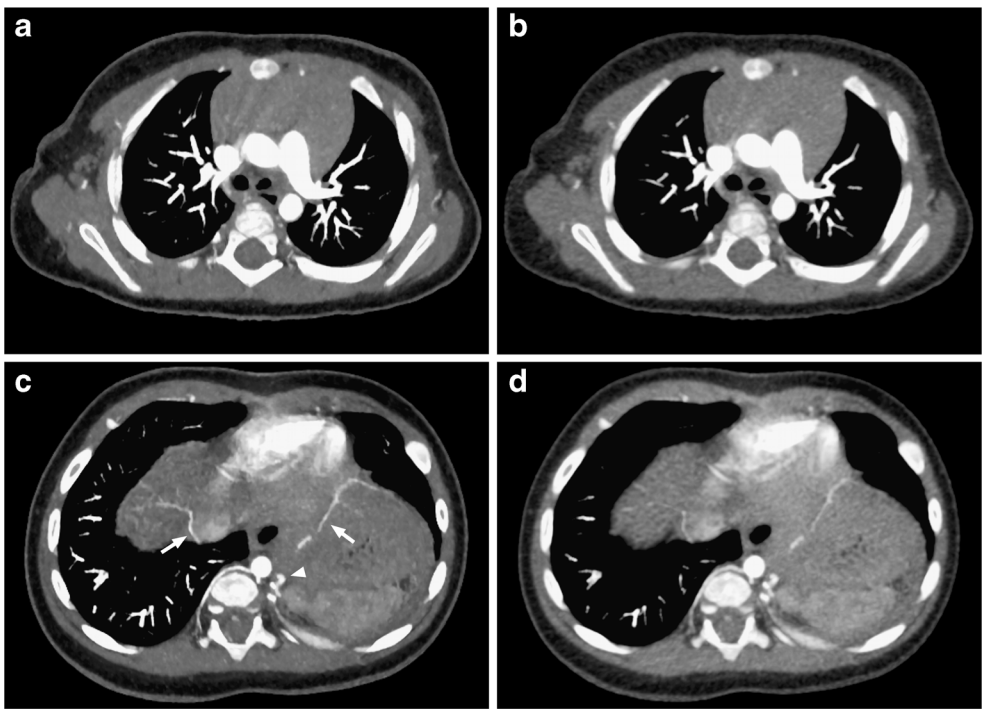

Fig. 1 A 6-month-old girl referred to CT for further work-up of a prenatal chest mass. Images are reconstructed with Veo™ (**a** and **c**) and ASIR™ (**b** and **d**) and are representative of the datasets used to make subjective assessments of the depiction of vascular structures, image noise and resolution of small anatomical structures. In addition to the pulmonary vessels, the small vessels in the upper abdomen and lower chest including the vessels feeding the chest mass/sequestration (*arrowhead*) and bilateral inferior phrenic arteries (*arrows*) are better delineated using the Veo™ algorithm (**c**). Image noise is also decreased for Veo™ in the visualized portions of the right lobe of the liver and spleen. The sequestration is not included on these images. For all images, window width and level values were kept constant, 600 and 155 Hounsfield units, respectively

Table 2 Subjective reader assessment of image quality. Each reader evaluated MBIR and ASIR™ images and then stated a preference for either MBIR or ASIR™ for the image quality category. Percentages represent the proportion of cases (n=17) where readers preferred MBIR images for better vessel definition, improved resolution of small anatomical structures and less apparent image noise (quantum mottle) over ASIR™

	Percentage of cases when MBIR preferred over ASIR™			
Image quality category	Reader 1	Reader 2	Reader 3	Reader 4
Vessel definition	100%	79%	94%	100%
Resolution of small structures	100%	94%	94%	100%
Image noise	100%	94%	94%	100%

clinical PACS workstation (AW Server 2; GE Healthcare, Milwaukee, WI). The length of each vessel was determined using 10-mm-thick axial maximum intensity projection images. The measure distance tool was implemented to perform measurement in mm from the vessel origin (i.e. main PA for the right upper lobe PA and aorta for the HA, SA and RA) to the most distal branch that could be reliably detected on the Veo™ and ASIR™ datasets. The identical distal branch was measured for both Veo™ and ASIR™ images. The visibly detectable terminal branches were counted for the apical segmental branch of the right upper lobe PA on both Veo™ and ASIR™ images. Some of the 17 chest cases also had z-coverage that included the upper abdominal viscera so we could reliably evaluate the small vessels in the liver, spleen and kidneys to count of the number of terminal branches and measure the lengths of the arteries supplying these organs. Specifically, the number of cases adequate to determine vessel length were the following: HA (n=6), SA (n=7), and RA (n=5).

Statistical analysis

Data were analyzed using Prism GraphPad software version 5.0d (La Jolla, CA). Differences in objective image noise and Hounsfield unit values were compared between Veo™ and ASIR™ datasets using the paired t-test. Differences between Veo™ and ASIR™ for the number of branches and vessel lengths were compared using Wilcoxon matched pairs signed rank test. Comparisons were considered significant when P<0.05.

Table 4 Comparison of vessel lengths (mean ± SD millimeters) on images created with model-based iterative reconstruction (MBIR) and adaptive statistical iterative reconstruction (ASIR™) algorithms

Vessel	MBIR	ASIR	P-value
Pulmonary artery	29.8±7.4	26.6±8.2	<0.0001
Hepatic artery	29.8±13.9	27.7±13.9	0.0313
Splenic artery	19.0±5.3	16.1±5.2	0.0156
Renal artery	17.5±5.4	14.2±4.7	0.0313

Results

CT scanner dose metrics for the 17 children were volume computed tomography dose index (CTDIvol)=3.05±1.19 (1.46 – 5.51) mGy and dose length product (DLP)=67.18± 43.69 (23.71 – 193.15) mGy-cm (mean ± standard deviation [range]). The overall image quality for the 17 studies was rated as good (4 out of 5) or excellent (5 out of 5) in all cases except one rated as adequate by one reader. This case rated as "adequate" (3 out of 5) had delayed bolus timing that resulted in an overall decrease vessel attenuation. The main drivers affecting overall image quality were patient motion (cardiac and respiratory). The four readers stated a subjective preference for Veo™ image quality over ASIR™ when rating image quality for vessel definition, resolution of small anatomical structures and relative absence of/less image noise (Table 2). Veo™ images consistently showed less image noise than ASIR™ for the aorta, fat and muscle; the quantitative analysis of image noise showed that the mean image noise measured in the aorta, subcutaneous fat and muscle were significantly different between Veo™ and ASIR™ images (Table 3).

Table 3 The average pixel Hounsfield unit (HU) and image noise as measured by the standard deviation (SD) of the HU-scale is compared at identical regions of interest for the contrast-enhanced lumen of the mid-thoracic aorta, paraspinal muscle and subcutaneous fat on images created with model-based iterative reconstruction (MBIR) and statistical iterative reconstruction (SIR) algorithms

Objective assessment of image noise						
	Average pixel (HU)			Standard deviation		
	MBIR	ASIR	P-value	MBIR	ASIR	P-value
Aorta	403.0±140.3	394.1±131.2	P<0.018	25.1±12.1	29.8±13.4	P<0.031
Fat	−122.2±16.6	−117.6±17.5	P<0.008	13.5±2.3	16.8±3.6	P<0.001
Muscle	62.2±10.4	62.1±11.3	P<0.96	13.4±1.9	19.2±7.0	P<0.004

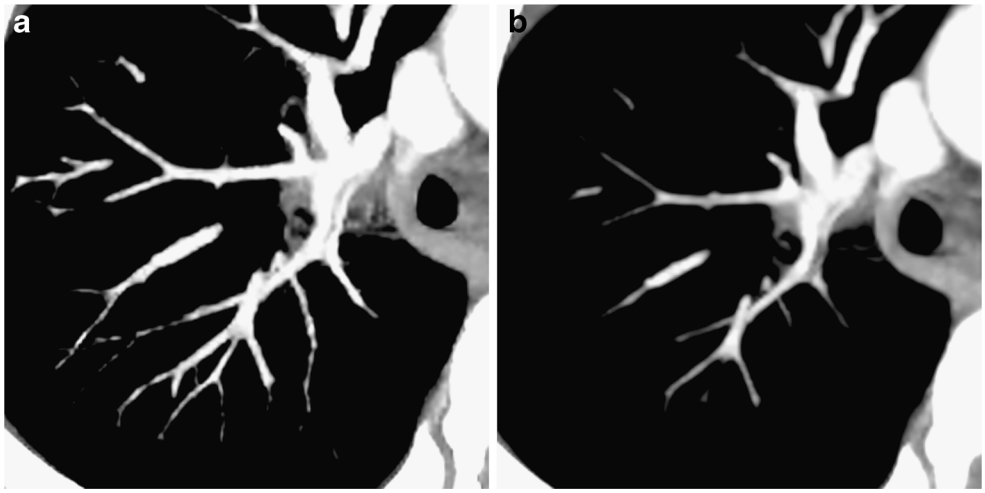

Fig. 2 A 5-year-old girl after liver transplantation and imaging obtained for evaluation of post-transplant lymphoproliferative disorder. Coned-down axial 10-mm maximum intensity projection images of the right hilum depict a greater number of pulmonary vessels and the vessels are visualized farther out into the periphery in the lung when images are created with Veo™ (**a**) than with ASIR™ (**b**). Both images are displayed with identical window width=400 Hounsfield units and window level=40 Hounsfield units

The quantitative analysis of vessel lengths showed that Veo™ images depicted PA, SA and RA vessels of longer lengths than on ASIR™ images (Table 4 and Fig. 2). Furthermore, the number of branch vessels depicted in the apical segment of the right upper lobe PA was consistently greater in number for each subject (Fig. 3) and significantly different on Veo™ (mean number of branch vessels ± standard deviation= 8.7±2.5) vs. ASIR™ (4.3±1.7, $P<0.0003$). This better depiction of branch vessels by Veo™ was also well visualized on volume-rendered images (Fig. 4). Vessel tracking also illustrated how Veo™ provided an improved depiction in the terminal vessels with less noise and less variation in luminal size (Fig. 5).

Discussion

This study evaluates the ability of two image reconstruction algorithms to resolve small vessels for pediatric CT imaging.

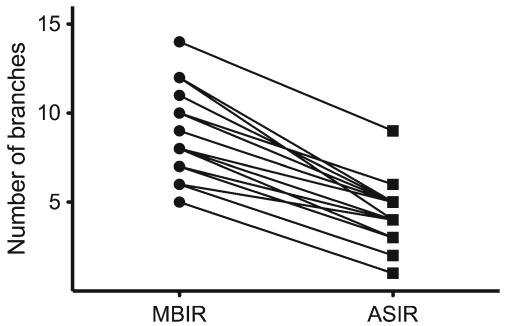

Fig. 3 Comparison of image reconstruction on number of branches visualized in the apical segmental branch of the right upper lobe pulmonary artery by Veo™ and ASIR™ algorithms. Each line connects data points for the number of branches counted on Veo™ and ASIR™ images for the same patient. All 17 patients have more branch vessels visualized on Veo™ than on ASIR™

We examine several objective and subjective measures of image quality and vessel depiction. The results indicate a significant improvement in the depiction of small vessel anatomy on images created using Veo™ over the more established ASIR™. Although noise reduction most likely plays a part, it is probable that the improvement in vessel depiction is largely attributable to the increased spatial resolution that has been observed with Veo™ [13, 14]. As in other clinical studies, however, it is not possible to establish this definitively, as spatial resolution was not measured directly [9, 10].

Reconstruction techniques for clinical CT continue to evolve in image quality, dose reduction and speed [12, 16, 17]. ASIR™ uses matrix algebra for the specific detection of image noise and subtracts the image quantum noise to achieve better image quality at reduced exposure compared to filtered back projection algorithm [12]. The Veo™ reconstruction engine represents a further step in iterative reconstruction technology by modeling the entire geometry of machine [13, 18–21].

Previous studies have examined noise by measuring the standard deviation of the Hounsfield units as an objective measure of image quality [18, 22]. We also found that Veo™ appears to decrease image noise in the aorta and subcutaneous fat. The factors that helped decrease noise in some tissues but not others might be related to the inherent variability in the densities of these tissues but would require further study to understand the differences in tissue noise produced by these reconstruction algorithms. The subjective measure of noise by the four readers also supported a benefit by Veo™. Readers preferred the depiction of vessel anatomy on Veo™ images.

Objective vessel analysis performed on two image sets showed that Veo™ was superior in depicting the vascular structures with more branches and longer in size than ASIR™. Since the spatial resolution increases with the implementation of Veo™ [23] this could translate into better conspicuity of

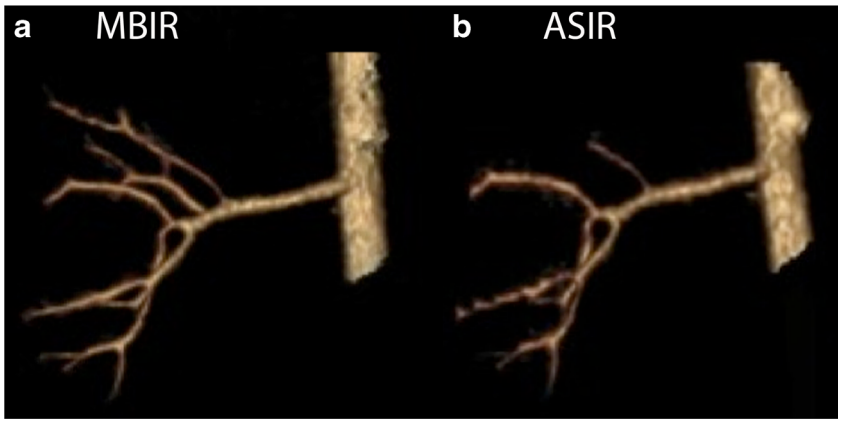

Fig. 4 A 7-year-old girl with anaplastic large cell lymphoma and status post left nephrectomy. The volume-rendered image of the right renal artery created from thin-slice data using the Veo™ algorithm (**a**) shows an increased number of branches that extend out farther into the periphery than on the VR image produced from thin-slice ASIR™ data (**b**)

small branches of vessels on the Veo™ images compared with ASIR™. Increased noise reduction capacity of Veo™ as shown in several previous studies [18, 20–22] in combination with better spatial resolution [13, 14] are additional explanations for why Veo™ appears to confer better vessel definition.

Contrast-enhanced CT has been validated by many studies for its diagnostic accuracy to detect vascular pathologies in adults and children [24, 25]; however, we know of no other study to date that evaluates the diagnostic efficacy of different reconstruction algorithms for the depiction of pediatric vessels using a CT protocol tailored to pediatric patients. Several previous studies for chest CT in adult patients show that Veo™ helps reduce radiation dose and improves image quality by reducing noise when compared to ASIR™ [13, 26]. In addition, several studies have examined how Veo™ improves the depiction of blood vessels using in vitro modeling [18] and when imaging the blood supply in the adult posterior fossa and spinal cord [19, 27]. For pediatric patients, Veo™ may be implemented in future studies to detect vascular abnormalities more accurately such as arteriovenous malformations, vascular supply of masses such as congenital foregut malformations (sequestration and congenital pulmonary airway malformation), and detection of pulmonary embolus.

Conducting a prospective study in a pediatric patient group with multiple scans at different radiation doses for both algorithms is ethically implausible, hence our current study is based on benchmarking adaptive and pure statistical methods in the same dataset; two image sets from one patient scan are created, one image set with ASIR™ and the other with Veo™. A potential benefit of CT imaging performed in conjunction with Veo™ is radiation dose reduction for children [15, 28]. If Veo™ can demonstrate conclusively improved image quality and decreased noise compared to ASIR™, Veo™ may also provide an opportunity to test dose reduction strategies while maintaining image quality. Further work will need to be done to evaluate whether this improvement in image quality translates into measureable differences in outcome for pediatric patients.

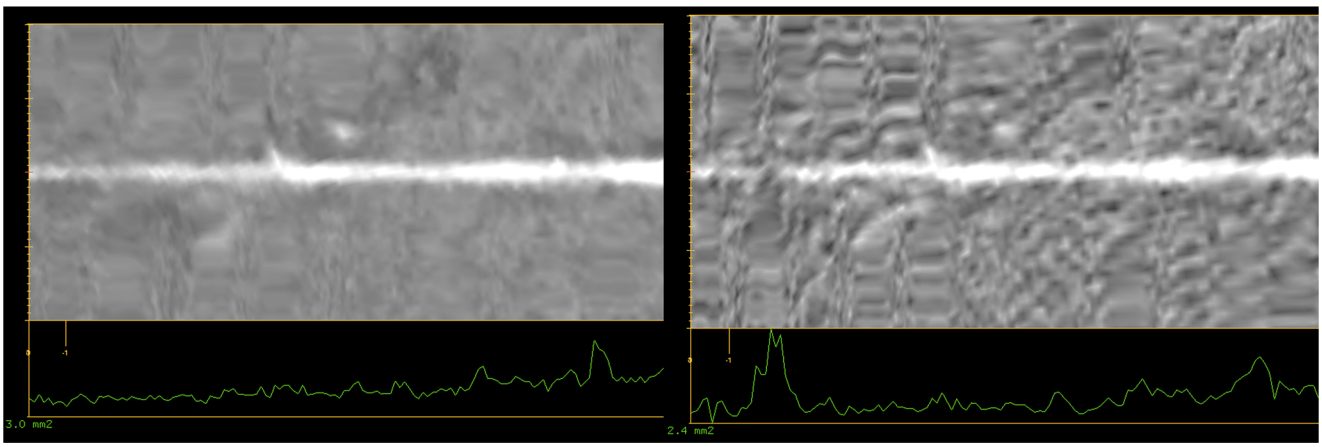

Fig. 5 A 7-month-old boy with congenital pulmonary airway malformation. The identical location of a peripheral branch of the right hepatic artery was tracked using thin-slice images obtained from Veo™ (**a**) and ASIR™ (**b**) algorithms. The dataset created with Veo™ produces vessel-tracking images with visibly less noise; also, the graph of estimated luminal diameter (shown below each image of the tracked vessel) has considerably less variation with Veo™

This study has several limitations to be considered. The subjective and objective aspects of the study are an attempt to characterize and quantify image quality, a complex area of image evaluation that is difficult to perform with current methodology under the best of circumstances. The approach using Hounsfield units and standard deviation are currently the method for image evaluation used by other scientific publications [14] but technically speaking is not a true definition of image noise. Also, MBIR and ASIR™ fundamentally change the nature of noise and a more sophisticated analysis beyond a simple ROI analysis as performed by Brady et al. [29] may be more appropriate. The study has a relatively small sample size and further work should be done to support and validate this preliminary data. Another limitation is that only one blend of ASIR™ at 30% was used as this is the preferred ASIR™ percentage at our institution. Several studies have focused on diagnostic efficacy and noise reduction potential of 20–100% blended ASIR™ reconstruction for a variety of imaging scenarios including coronary, cranial and chest CT imaging [11, 30], but no consensus exists for the appropriate blending percentage of ASIR™. Only five-seven cases had imaging to evaluate abdominal vessels; however, even with this small sample size the performance of Veo™ appears to confer a distinct advantage for vessel depiction of the hepatic, splenic and renal arteries. The relatively long period of time required to process and create images using the current version of the Veo™ software package is on the order of 30–60 min whereas ASIR™ images can usually be created in less than 1 min. This delay could impact patient care, particularly in emergency situations. However, this reconstruction time will likely decrease substantially in-step with continued advances in computer technology. Another shortcoming of the study emerged during the qualitative image assessment; although we removed study info from the Veo™ and ASIR™ datasets to blind the readers during their subjective assessments, the inherent smoothing effect of Veo™ on the appearance of CT images limited a true blinding. Thus, the inherent differences between Veo™ and ASIR™ in the way the images look will likely lead to some bias.

Conclusion

Our study demonstrates that model-based iterative reconstruction using Veo™ provides improved depiction of vessel anatomy with decreased image noise in a small pediatric patient population. This technology holds promise for more precise depiction of small anatomical structures in children, at comparable radiation dose and potentially reduced radiation dose compared to established adaptive statistical iterative reconstruction.

Conflicts of interest None

References

1. Epelman M, Kreiger PA, Servaes S et al (2010) Current imaging of prenatally diagnosed congenital lung lesions. Semin Ultrasound CT MR 31:141–157
2. O'Connor OJ, Vandeleur M, McGarrigle AM et al (2010) Development of low-dose protocols for thin-section CT assessment of cystic fibrosis in pediatric patients. Radiology 257:820–829
3. Alibek S, Brand M, Suess C et al (2011) Dose reduction in pediatric computed tomography with automated exposure control. Acad Radiol 18:690–693
4. Lell MM, May M, Deak P et al (2011) High-pitch spiral computed tomography: effect on image quality and radiation dose in pediatric chest computed tomography. Invest Radiol 46:116–123
5. Winklehner A, Karlo C, Puippe G et al (2011) Raw data-based iterative reconstruction in body CTA: evaluation of radiation dose saving potential. Eur Radiol 21:2521–2526
6. Fuchs TA, Fiechter M, Gebhard C et al (2012) CT coronary angiography: impact of adapted statistical iterative reconstruction (ASIR™) on coronary stenosis and plaque composition analysis. Int J Cardiovasc Imaging 29:719–724
7. Baumueller S, Winklehner A, Karlo C et al (2012) Low-dose CT of the lung: potential value of iterative reconstructions. Eur Radiol 22: 2597–2606
8. Katsura M, Sato J, Akahane M et al (2012) Comparison of pure and hybrid iterative reconstruction techniques with conventional filtered back projection: Image quality assessment in the cervicothoracic region. Eur J Radiol 82:356–360
9. Deak Z, Grimm JM, Treitl M et al (2013) Filtered back projection, adaptive statistical iterative reconstruction, and a model-based iterative reconstruction in abdominal CT: an experimental clinical study. Radiology 266:197–206
10. Pickhardt PJ, Lubner MG, Kim DH et al (2012) Abdominal CT with model-based iterative reconstruction (MBIR): initial results of a prospective trial comparing ultralow-dose with standard-dose imaging. AJR Am J Roentgenol 199:1266–1274
11. Beister M, Kolditz D, Kalender WA (2012) Iterative reconstruction methods in X-ray CT. Phys Med 28:94–108
12. Silva AC, Lawder HJ, Hara A et al (2010) Innovations in CT dose reduction strategy: application of the adaptive statistical iterative reconstruction algorithm. AJR Am J Roentgenol 194:191–199
13. Katsura M, Matsuda I, Akahane M et al (2012) Model-based iterative reconstruction technique for radiation dose reduction in chest CT: comparison with the adaptive statistical iterative reconstruction technique. Eur Radiol 22:1613–1623
14. Mieville FA, Berteloot L, Grandjean A et al (2013) Model-based iterative reconstruction in pediatric chest CT: assessment of image quality in a prospective study of children with cystic fibrosis. Pediatr Radiol 43:558–567
15. Smith EA, Dillman JR, Goodsitt MM et al (2013) Model-based iterative reconstruction: effect on patient radiation dose and image quality in pediatric body CT. Radiology. doi:10.1148/radiol.13130362 [Epub ahead of print]
16. Brooks RA, Di Chiro G (1976) Principles of computer assisted tomography (CAT) in radiographic and radioisotopic imaging. Phys Med Biol 21:689–732
17. Hounsfield GN (1973) Computerized transverse axial scanning (tomography). 1. Description of system. Br J Radiol 46:1016–1022

18. Suzuki S, Machida H, Tanaka I et al (2012) Measurement of vascular wall attenuation: comparison of CT angiography using model-based iterative reconstruction with standard filtered back-projection algorithm CT in vitro. Eur J Radiol 81: 3348–3353
19. Machida H, Tanaka I, Fukui R et al (2013) Improved delineation of the anterior spinal artery with model-based iterative reconstruction in CT angiography: a clinical pilot study. AJR Am J Roentgenol 200: 442–446
20. Singh S, Kalra MK, Do S et al (2012) Comparison of hybrid and pure iterative reconstruction techniques with conventional filtered back projection: dose reduction potential in the abdomen. J Comput Assist Tomogr 36:347–353
21. Scheffel H, Stolzmann P, Schlett CL et al (2012) Coronary artery plaques: cardiac CT with model-based and adaptive-statistical iterative reconstruction technique. Eur J Radiol 81: e363–e369
22. Yoon MA, Kim SH, Lee JM et al (2012) Adaptive statistical iterative reconstruction and Veo™ : assessment of image quality and diagnostic performance in CT colonography at various radiation doses. J Comput Assist Tomogr 36:596–601
23. Yu Z, Thibault JB, Bouman CA et al (2011) Fast model-based X-ray CT reconstruction using spatially nonhomogeneous ICD optimization. IEEE Trans Image Process 20:161–175
24. Willems PW, Taeshineetanakul P, Schenk B et al (2012) The use of 4D-CTA in the diagnostic work-up of brain arteriovenous malformations. Neuroradiology 54:123–131
25. Kritsaneepaiboon S, Lee EY, Zurakowski D et al (2009) MDCT pulmonary angiography evaluation of pulmonary embolism in children. AJR Am J Roentgenol 192:1246–1252
26. Neroladaki A, Botsikas D, Boudabbous S et al (2013) Computed tomography of the chest with model-based iterative reconstruction using a radiation exposure similar to chest X-ray examination: preliminary observations. Eur Radiol 23:360–366
27. Machida H, Takeuchi H, Tanaka I et al (2013) Improved delineation of arteries in the posterior fossa of the brain by model-based iterative reconstruction in volume-rendered 3D CT angiography. AJNR Am J Neuroradiol 34:971–975
28. Singh S, Kalra MK, Shenoy-Bhangle AS et al (2012) Radiation dose reduction with hybrid iterative reconstruction for pediatric CT. Radiology 263:537–546
29. Brady SL, Yee BS, Kaufman RA (2012) Characterization of adaptive statistical iterative reconstruction algorithm for dose reduction in CT: a pediatric oncology perspective. Med Phys 39:5520–5531
30. Rapalino O, Kamalian S, Kamalian S et al (2012) Cranial CT with adaptive statistical iterative reconstruction: improved image quality with concomitant radiation dose reduction. AJNR Am J Neuroradiol 33:609–615